within a solid planetary body as large as Io is transported by solid-state convection. The uniform heating rate that would be necessary to maintain a temperature difference ΔT across a solid convecting layer of mantle can be estimated by the relation $H = (0.4)\Delta T k R_a^{1/4}/L^2$. Here L is the mantle thickness, k is the thermal conductivity, and R_a is the Rayleigh number $\alpha g L^5 H/2k\kappa\nu$ (g, α, κ, and ν are the gravitational acceleration thermal expansion coefficient, thermal diffusivity, and kinematic viscosity, respectively). This formula is based on both experimental data (*9*) and numerical calculations with spherical geometry (*10*). Its application to problems of planetary heat transfer is discussed in detail by Schubert *et al.* (*11*).

Suppose that, for $L = R_s$ (no liquid core) and ΔT equal to that necessary for melting at the center of the satellite, H was just equal to H_0, the mean tidal heating rate for a solid Io. Then H/H_0 is approximately R_s/L for all L, since ΔT and the other parameters would not vary appreciably with L. Figure 2 shows $H/H_0 = R_s/L$. Also plotted in Fig. 2 is H_T, the mean tidal dissipation rate in the mantle, also normalized by H_0. As the core radius increases, heating due to tidal dissipation exceeds by an increasing amount the energy that can be removed by solid-state convection. By comparison with the moon, it seems likely that $H/H_0 < 1$ for $L = R_s$, in which case the dashed curve in Fig. 2 would lie even farther below the curve of H_T/H_0. Thus, solid convection cannot prevent the melting from rapidly spreading through the rest of the satellite once melting has occurred at the center.

The result of this runaway melting process is a planet with a large molten core and a solid outer shell, the thickness of which is limited by conduction of the internally generated heat to the surface, or possibly by the onset of nonelastic behavior such as fracture. Conduction-limited runaway would result in a thin shell indeed. The solid curve in Fig. 2 reaches an upper limit of 500, which was calculated by using the shell equations derived by Peale and Cassen (*2*). Then for conductive equilibrium of the shell, $H/H_0 = 2k\Delta T/H_0L^2$. With $k = 4 \times 10^5$ erg/cm-sec-K and $\Delta T = 1300$ K, the thickness L would be 18 km. The periodic component of the tide in this nearly fluid satellite would have a maximum amplitude of 100 m.

The implications of the orbital resonances of the inner three Galilean satellites are profound for the thermal state of Io. These calculations suggest that Io might currently be the most intensely heated terrestrial-type body in the solar system. The surface of the type of body postulated here has not yet been directly observed, and although the morphology of such a surface cannot be predicted in any detail, one might speculate that widespread and recurrent surface volcanism would occur, leading to extensive differentiation and outgassing (*12*). Transient infrared brightening of Io has recently been observed (*13*). Surface magmatic events might produce such brightening. The appearance of craters produced by events of sufficient energy to penetrate the crust should be different from those on bodies with thick, solid mantles. The question of distinguishing between a solid mantle and a liquid mantle with a thin crust is important for the outer icy satellites as well as for Io. Although this structural model of Io is analogous to the solid crust-liquid mantle model proposed for the large icy satellites (*14*), it has recently been shown that the hypothetical liquid mantle of these satellites would be solidified by solid-state convection in the icy crust (*15*). Finally, cosmic elemental abundance ratios, the density of Io, and the high internal temperatures would imply a molten iron core with a radius perhaps one-third that of Io. Therefore, by analogy with Earth, the satellite might have a magentic field, the interaction of which with the jovian magnetosphere would be the source of interesting plasma phenomena. Voyager images of Io may reveal evidence for a planetary structure and history dramatically different from any previously observed.

S. J. PEALE

Department of Physics, University of California, Santa Barbara 93106

P. CASSEN
R. T. REYNOLDS

Theoretical and Planetary Studies Branch, NASA-Ames Research Center, Moffett Field, California 94035

References and Notes

1. W. de Sitter, *Ann. Leiden Obs.* **16**, part 2 (1928).
2. S. J. Peale and P. Cassen, *Icarus* **36**, 240 (1978).
3. W. de Sitter, *Mon. Not. R. Astron. Soc.* **91**, 706 (1931).
4. A. Sinclair, *ibid.* **171**, 59 (1975).
5. J. Lieske, private communication.
6. P. Goldreich and S. Soter, *Icarus* **5**, 375 (1966).
7. P. Cassen, R. T. Reynolds, F. Graziani, A. Summers, J. McNellis, L. Blalock, *Phys. Earth Planet. Inter.*, in press.
8. Y. Nakamura, G. V. Latham, H. J. Dorman, F. K. Duennebier, *Proc. 7th Lunar Sci. Conf.* (1976), p. 3113.
9. F. A. Kulacki and A. A. Emara, *J. Fluid Mech.* **83**, 375 (1977).
10. R. E. Young, *ibid.* **63**, 695 (1974).
11. G. Schubert, P. Cassen, R. E. Young, *Icarus*, in press.
12. F. P. Fanale, T. V. Johnson, D. L. Matson, in *Planetary Satellites*, J. A. Burns, Ed. (Univ. of Arizona Press, Tucson, 1977).
13. F. C. Witteborn, J. D. Bregman, J. B. Pollack, *Science* **203**, 643 (1979).
14. J. Lewis, *ibid.* **172**, 1127 (1971).
15. R. T. Reynolds and P. Cassen, *J. Geophys. Res. Lett.* in press.
16. We gratefully acknowledge discussions with R. Greenberg and J. Lieske and thank the latter for kindly furnishing a computer printout of his calculations of the Galilean satellite motions. S.J.P. is supported in this research by NASA grant NGR 05-010-062 and by NASA-Ames Research Center under interchange NCA-2-OR680-701.

26 January 1979

Anomalous Bottom Water South of the Grand Banks Suggests Turbidity Current Activity

Abstract. *Highly turbid bottom water at the margin of the Sohm Abyssal Plain was identified by its temperature, salinity, and oxygen content as originating upslope on the continental rise. The fact that the particulate concentrations were one to two orders of magnitude higher than are normally found in deep ocean waters suggests a turbidity current as the agent bringing this water downslope.*

In 1952 Heezen and Ewing (*1*) showed that submarine telegraph cables must have been severed by a massive turbidity current that developed after the 1929 Grand Banks earthquake rather than as the result of the direct action of earth shocks, as had been supposed. Although it is doubtful that turbid water remains from that particular event, muddy water has been photographed at the bottom in the Sohm Abyssal Plain, presumably from more recent turbidity current events in the same region (*2*).

Near-bottom water samples collected south of the Grand Banks in 1971 contained an unusually high concentration of suspended particulate matter. Many hundreds of light-scattering profiles have been obtained in Atlantic Ocean waters, and the broad-scale horizontal and vertical distribution of particulate matter has been mapped from these data (*3*). Our 1971 measurements are truly anomalous when compared to this overall distribution, and in light of some recent data collected in the same region (*4-7*) we report here on our reexamination of the 1971 data.

The bottom waters overlying the western margins of the North and South Atlantic basins contain high concentrations of suspended particulate material. Concentrations of more than 200 μg liter^{-1} have been measured (*8, 9*), making these regions among the most highly "turbid" of deep ocean waters (*3*). At the level of clearest water, at a depth of about 3000 m in the Atlantic Ocean, the concentration can be less than 10 μg liter^{-1} (*3, 9*), whereas in the turbid waters of the continental shelves the values may exceed 1000 μg liter^{-1} (*10*). Johnson and Lonsdale (*4*) reported that on the New England continental rise near Mytilus Seamount their deep-tow camera view of the ocean floor was completely obscured by backscatter from suspended particulates (they did not measure particulate concentrations). All but the largest features normally visible in conventional ocean-bottom photographs are obscured in waters containing 200 μg of suspended particulate matter per liter, and 500 μg liter^{-1} obscures the bottom completely (*11*).

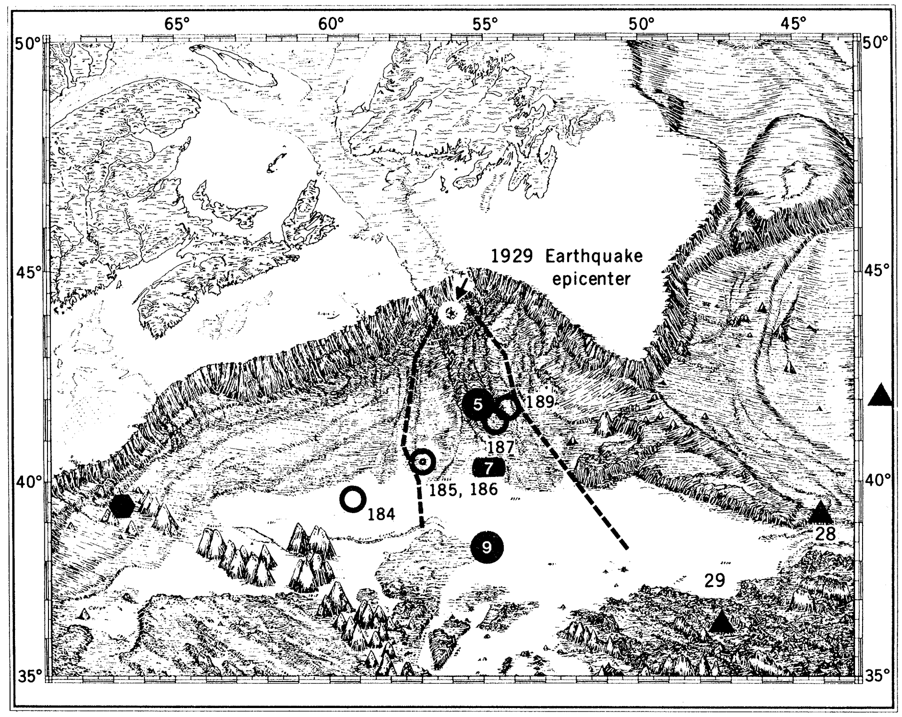

Fig. 1. Location of the *Lynch* 47 stations (open circles) on a physiographic diagram (*15*) of the Sohm Abyssal Plain–Grand Banks region of the North Atlantic. The dashed lines show channels through which the 1929 Grand Banks turbidity current flowed (*1*). Triangles are GEOSECS station locations (*5, 6*). Closed circles are Polymode station locations. The hexagon shows a region of very turbid bottom water near Mytilus Seamount (*4*).

At 40°26.2′N, 56°55.8′W (station *Lynch* 47-186) in 5200 m of water at the edge of the Sohm Abyssal Plain (Fig. 1), near-bottom water samples contained an unusually high concentration of particulate material as measured by a laboratory turbidimeter (Hach model 2100A). All samples collected were being analyzed as an experiment to see if the turbidimeter could be used to give a measure of the distribution of suspended particulates in deep ocean waters. In a later study in the North American basin, Biscaye and Eittreim (*8*) calibrated the same model turbidimeter against large-volume seawater samples filtered on shipboard and analyzed gravimetrically in the laboratory for particulates. The anomalous *Lynch* values (Fig. 2a) exceed the upper limit of Biscaye and Eittreim's calibration data (180 μg liter^{-1}). A laboratory calibration of another Hach model 2100A turbidimeter based on the use of dry weights of pelagic clays suspended in filtered deionized water showed the instrument to be nonlinear at particulate concentrations less than a few hundred micrograms per liter (where almost all deep-ocean values occur) but linear in the range from 1000 to 10,000 μg liter^{-1}. Nonetheless, the results (Fig. 2a) give an idea of the general distribution of suspended particulates in the ocean: that is, high surface values due to the presence of planktonic organisms, a broad minimum throughout midwater depths, and a turbid bottom boundary layer. Figure 2a also shows the dramatic values obtained in the bottom 50 m of station 186 and for the one good sample at nearby station 185 (*12*). Particulate concentrations range from 1500 to 4000 μg liter^{-1} (or 6000 to 16,000 μg liter^{-1}, if the laboratory calibration is used). These values are one to two orders of magnitude higher than those normally found in deep ocean waters. Adjacent stations 184 and 187 also showed values higher than normal, 150 to 300 μg liter^{-1} (500 to 1200 μg liter^{-1}, if the laboratory calibration is used).

A suspension of 10 mg of pelagic clay in a liter of water (10,000 μg liter^{-1}) appears only slightly turbid when viewed in a glass container in normal interior lighting and could go unnoticed during routine shipboard water sampling and analysis procedures.

Other features of the near-bottom water column at station 186 were also anomalous (Fig. 2b): in the bottom 50 m, temperature, salinity, and the dissolved oxygen content increased. The bottom boundary layer in the western North Atlantic basin can usually be seen in the water structure as a layer of nearly homogeneous water above the bottom varying in thickness from tens to hundreds of meters and capped by a benthic thermocline. Almost exclusively, the water in this layer is colder and less saline than that above it (*13*); in contrast, at station 186 the opposite is true. Two Geochemical Ocean Section Study (GEOSECS) stations (No. 28, and to a certain extent No. 27; see Fig. 1) also show a steplike increase in salinity, temperature, dissolved oxygen content, and light-scattering near the bottom (*5, 6*). The bottom water at station 186 has the properties of water found about 1000 m higher up in the same water column (Fig. 2b) and tends toward the characteristics of water found at the bottom on the continental rise at station 189 which has significant admixtures of Denmark Strait water (see Fig. 2c). Station 187 is intermediate between stations 186 and 189.

We believe that the anomalous bottom water at station 186 is the result of lateral (downslope) advection rather than vertical mixing. The water column at station 186 is in stable equilibrium because the adiabatic temperature gradient exceeds the in situ gradient (Fig. 2b) except in the bottom discontinuity where vertical stability is maintained by the salinity increase.

Others have proposed lateral advection as a mechanism for creating the observed interleaving of water masses in the bottom boundary in this region (*5-7*). We suggest that at station 186 the anomalous water once resided higher up on the continental margin and was brought downslope by entrainment during a turbidity current event in this historically active area. The addition of the suspended particulate matter, assuming a particle density of 2 g cm^{-3}, would increase the water density by as much as 0.01 σ_t unit (0.00001 g cm^{-3}), further enhancing the stability of the bottom layer.

Currents measured 1.5 m above the

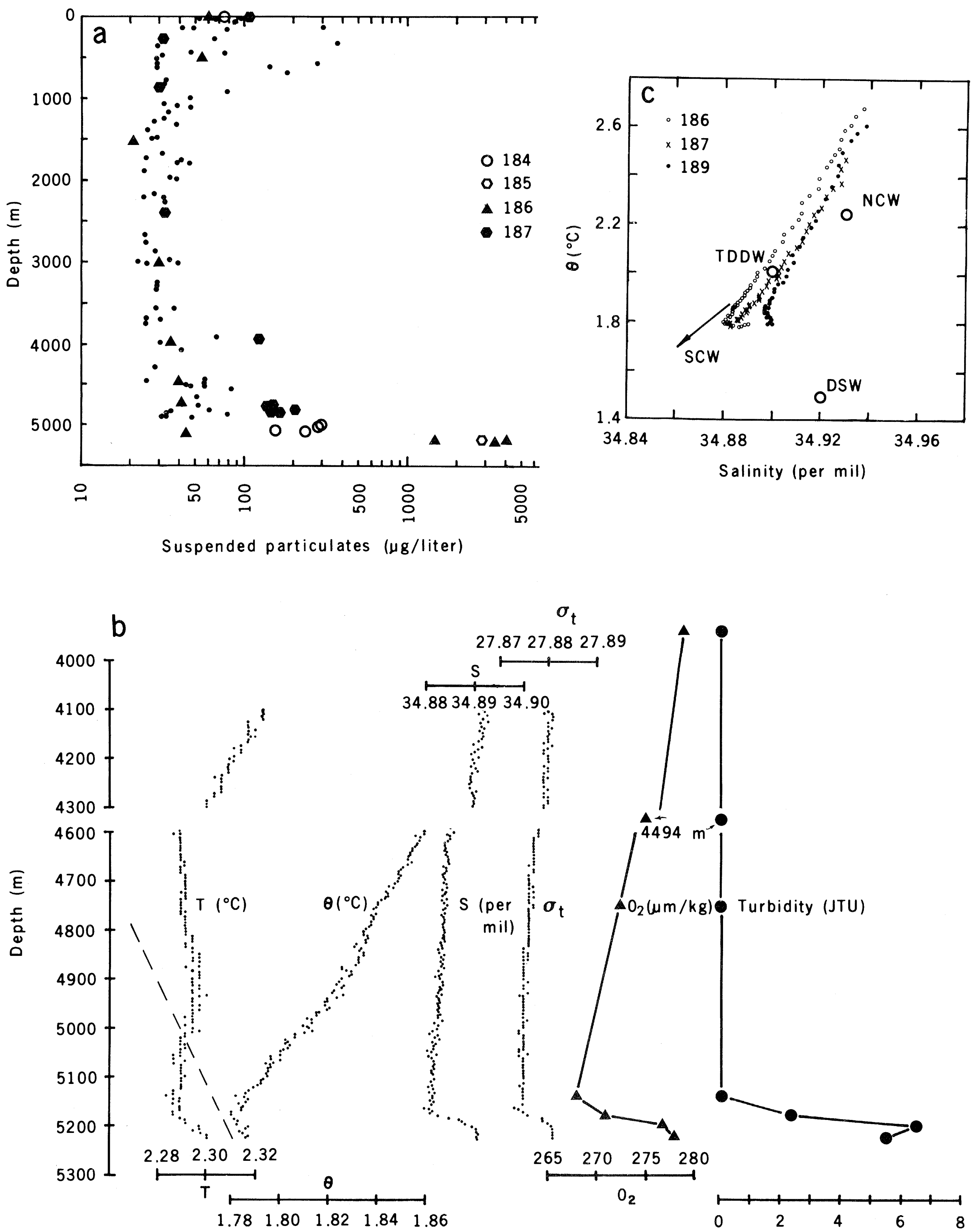

Fig. 2. (a) Distribution of suspended particulate material in the Sohm Abyssal Plain in May 1971. Stations where very high bottom values were found are identified by symbols. Samples were analyzed in vitro with a turbidimeter and converted to micrograms per liter on the basis of Biscaye and Eittreim's (*8*) calibration curve. The suspended particulates are plotted on a logarithmic scale. (b) Near-bottom vertical profiles of in situ temperature (*T*), potential temperature (θ), salinity (*S*), σ_t, dissolved O_2, and turbidity at station 186. The *T*, θ, *S*, and σ_t values were obtained from continuously recorded salinity-temperature-depth (STD) sensor data (Bissett-Berman model 9006). The O_2 and turbidity data were measured in water samples collected simultaneously with the STD cast. The break in the depth scale shows how the values of *S*, *T*, σ_t, and dissolved O_2 content at the ocean bottom are also found from 4100 to 4300 m in the same water column. Turbidity is measured in Jackson turbidity units (*JTU*) (*16*), the actual units of turbidity measured on the Hach model 2100A turbidimeter; we have converted these values to particulate concentrations in the text. The hatched line is the adiabatic gradient (0.096°C per kilometer). (c) A θ/S diagram for stations 186, 187, and 189. The water mass abbreviations are as follows: *NCW*, northern component water; *TDDW*, 2-degree discontinuity water; *DWS*, Denmark Strait water; and *SCW*, southern component water (the arrow points to its off-scale location of −0.1°C, 34.67 per mil) (*5*).

bottom at station 185 (15 km northeast of station 186) averaged 23 cm sec^{-1} toward 300° during the time measurements were being taken at station 186 and averaged 2.3 cm sec^{-1} toward the east at station 187. These observations lasted for only half a semidiurnal tidal cycle and do not represent the average current regime in the region. The main deep current in this region is the Western Boundary Undercurrent (WBUC). The southwesterly trending WBUC might well transport such patches of turbid water along the continental margin after the turbidity flow has expended most of its forward momentum near the edge of the abyssal plain.

Seismograph records at Lamont-Doherty Geological Observatory have been examined for the period 25 April to 8 May 1971 (2 weeks prior to the date of the measurements made at station 186) for evidence of significant seismic activity in the Grand Banks area. No such activity was detected (*14*).

We believe that other isolated patches of highly turbid bottom water that have been found along the western margin of the North American basin should also be considered in this light (*4–8*). It may not be necessary to have very high bottom currents actively eroding the substrate at the site of observation to account for the high concentrations of particulate matter in some bottom waters.

ANTHONY F. AMOS
Port Aransas Marine Laboratory, University of Texas Marine Science Institute, Port Aransas 78373
ROBERT D. GERARD
Lamont-Doherty Geological Observatory, Columbia University, Palisades, New York 10964

References and Notes

1. B. C. Heezen and M. Ewing, *Am. J. Sci.* **250**, 849 (1952).
2. B. C. Heezen and C. D. Hollister, *The Face of the Deep* (Oxford Univ. Press, New York, 1971), pp. 283–333.
3. P. E. Biscaye and S. L. Eittreim, *Mar. Geol.* **23**, 155 (1977).
4. D. A. Johnson and P. F. Lonsdale, *Deep-Sea Res.* **23**, 429 (1976).
5. W. S. Broecker, T. Takahashi, Y.-H. Li, *ibid.*, p. 1083.
6. W. S. Broecker and A. Bainbridge, *J. Geophys. Res.* **83**, 1963 (1978).
7. L. Armi, *ibid.*, p. 1971.
8. P. E. Biscaye and S. L. Eittreim, in *Suspended Solids in Water*, R. Gibbs, Ed. (Plenum, New York, 1974), p. 227.
9. P. G. Brewer, D. W. Spencer, P. E. Biscaye, A. Hanley, P. L. Sachs, C. L. Smith, S. Kadar, J. Fredericks, *Earth Planet. Sci. Lett.* **32**, 393 (1976).
10. P. E. Biscaye and C. R. Olsen, *Am. Soc. Limnol. Oceanogr. Spec. Symp.* **2**, 124 (1976).
11. A. F. Amos, *The New York Bight and Hudson Canyon in October 1974* (Technical Report COO-2185-10, Lamont-Doherty Geological Observatory, Palisades, N.Y., 1976), pp. 150–180.
12. An acoustic "pinger" was used to prevent our instrument package from touching bottom and stirring up sediment. Two of the highly turbid samples (station 186) were collected in bottles attached to the wire above our STD instrument, one sample (station 186) was collected in a "rosette" sampler bottle surrounding the STD, and one sample (station 185) was collected 15 km away. Thus, contamination of stirred-up sediment is improbable. The closest approach to the bottom at station 186 was 4 m.
13. A. F. Amos, A. L. Gordon, E. D. Schneider, *Deep-Sea Res.* **18**, 145 (1971); L. Armi and R. C. Millard, *J. Geophys. Res.* **81**, 4983 (1976).
14. L. Sykes, personal communication.
15. B. C. Heezen and M. Tharp, *Physiographic Diagram of the North Atlantic Ocean* (Geological Society of America map, Boulder, Colo., 1968).
16. Anonymous, *Proceedings of the National Oceanographic Instrumentation Center Turbidity Workshop*, Washington, D.C., 6–8 May 1974.
17. We thank E. Escowitz and the Global Ocean Floor Analysis and Research group at the Naval Oceanographic Office, Chesapeake Beach, Md. (1971), facility who made available to us the U.S.N.S. *Lynch*. This work was supported by Energy Research and Development Administration contract AT(11-1) 2185. University of Texas Marine Science Institute contribution 306. Lamont-Doherty Geological Observatory contribution 2747.

7 July 1978; revised 11 September 1978

Generation of Oil-Like Pyrolyzates from Organic-Rich Shales

Abstract. *Pyrolyzates similar to natural crude oils were generated from organic-rich shales by hydrous pyrolysis. With this type of pyrolysis it is possible to make more sophisticated correlations between crude oils and their source rocks, evaluate the hydrocarbon potential of a source rock, and elucidate the variables involved in the natural oil-generating process.*

The products generated by anhydrous pyrolysis and retorting of organic-rich shales contain significant amounts of olefins (Fig. 1). The rarity of olefins in natural crude oils (*1*) indicates that these pyrolysis methods do not duplicate the natural oil-generating process. In June 1977 we generated pyrolyzates that did not contain olefins from organic-rich shales (Fig. 1). In addition, the pyrolyzates had other properties that closely match those of natural crude oils. The process, called hydrous pyrolysis, involves filling half of a pressure vessel with equal volumes of water and crushed or sawed blocks of organic-rich shale. The remaining void is filled with helium at 1 to 2 atm, and the vessel is then heated to 330°C for 3 to 4 days.

The organic-rich shales used in this process are in their prehydrocarbon generation stage of diagenesis. This is evaluated before pyrolysis by elemental analyses and visual analysis of the kerogen portion of the organic matter (*2–5*). Oil-like pyrolyzates have been generated by this process from shales containing algal and liptinitic kerogens. Woodford Shale from Carter County, Oklahoma, which contains liptinitic kerogen and 4.3 percent (by weight) organic carbon, is used in this report as an example of hydrous pyrolysis.

A gas chromatogram of the pyrolyzate generated by hydrous pyrolysis of Woodford Shale (Fig. 2A) is similar to that of a natural crude oil (Fig. 2B) that has been geochemically correlated (*6*)

Table 1. Comparison of natural crude oils with pyrolyzates generated by hydrous pyrolysis.

Substance	*n*-Alkane range	CPI*	Pristane/phytane ratio	Optical rotation	$\delta^{13}C$ (PDB)†
Natural Woodford crude oils	C_1 to C_{37}	1.0	1.4 to 1.5	0.1 to 0.3	−29.8 to −30.0
Pyrolyzates from hydrous pyrolysis of Woodford Shale	C_1 to C_{37}	1.0 to 1.1	1.1 to 2.3	0.1 to 0.2	−29.4 to −30.0
Crude oils (overall range)	C_1 to C_{37}	0.8 to 1.2	0.4 to 8.0	−0.1 to 4.5	−21.0 to −35.0

*Carbon preference index (CPI) = $\frac{1}{2}\,[(C_{25} + C_{27} + C_{29})/(C_{24} + C_{26} + C_{28}) + (C_{25} + C_{27} + C_{29})/(C_{26} + C_{28} + C_{30})]$. †Per mil increment in ^{13}C relative to Pee Dee belemnite.

Table 2. Composition of natural crude oils and pyrolyzates generated by hydrous pyrolysis at 330°C for 96 hours. Values are percentages by weight.

Substance	Eluted fraction* (%)				Non-eluted† fraction (%)
	Saturates	Aromatics	Polars	Total	
Natural Woodford crude oils	80–89	10–16	1–4	100	0
Pyrolyzates from hydrous pyrolysis of Woodford Shale	62	28	10	62	38

*Portion eluted on an activated alumina column with *n*-heptane (saturates), dichloromethane (aromatics), and dichloromethane-methanol mixtures (polars). †Portion not eluted on an activated alumina column with dichloromethane-methanol mixtures.

0036-8075/79/0302-0897$00.50/0